JACS
JOURNAL OF THE AMERICAN CHEMICAL SOCIETY

ARTICLE

pubs.acs.org/JACS

# Atomic Solid State Energy Scale

Brian D. Pelatt,[†] Ram Ravichandran,[†] John F. Wager,[†] and Douglas A. Keszler[*,‡]

[†]School of EECS, Oregon State University, 1148 Kelley Engineering Center, Corvallis, Oregon 97331-5501, United States
[‡]Department of Chemistry, Oregon State University, 153 Gilbert Hall, Corvallis, Oregon 97331-4003, United States

**ABSTRACT:** A plot of electron affinity (EA) and ionization potential (IP) versus energy band gap ($E_G$) for 69 binary closed-shell inorganic semiconductors and insulators reveals that $E_G$ is centered about the hydrogen donor/acceptor ionization energy $\varepsilon(+/-)$. Thus, $\varepsilon(+/-)$, or equivalently the standard hydrogen electrode (SHE) energy, functions as an absolute energy reference, determining the tendency of an atom to be either a cation or anion in a compound. This empirical trend establishes the basis for defining a new solid state energy (SSE) scale. This SSE scale makes possible simple approaches for quantitatively assessing electronegativity, chemical hardness, and ionicity, while also providing new insight into the periodic trends of solids.

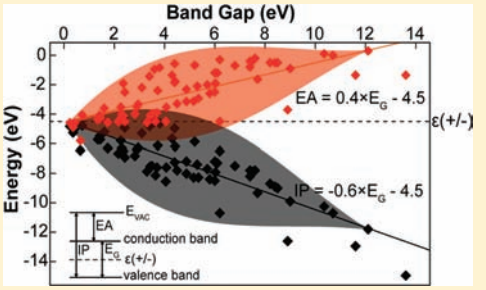


## INTRODUCTION

An understanding of the relative and absolute electronic energies of materials and molecules is required to successfully address many design problems in science. Knowledge of band offsets between two materials is critically important for creating new semiconductor devices, whereas awareness of the relative energies of solids and molecules facilitates the conception of new catalysts. In liquid solutions, these energies are quantitatively summarized as standard reduction potentials,[1] forming the foundation of electrochemistry. It is common to consider the periodic trends of these potentials in the context of other atomic concepts such as electronegativity. As we move to such concepts, however, the quantitative structure and utility blur, eventually limiting their widespread use.

Unlike standard reduction potentials for solutions, no simple model has been recognized for quantitative assessment and prediction of electronic energies of solids and their periodic tendencies. In this contribution, we describe an empirical method for estimating these quantities and establishing trends. This technique provides a unified approach to solid state energies, solution-based reduction potentials, and several foundational concepts in chemistry and allied disciplines.

## METHODS

Literature values for ionization potential (IP) and energy gap ($E_G$) are used to define the absolute energies of electronic levels in solids according to the insert of Figure 1. IP values from photoemission experiments set the valence-band maximum energy, and optical measurements of $E_G$ are then used to derive the electron affinity (EA), setting the conduction-band minimum energy. IP, $E_G$, and EA data for 69 closed-shell binary inorganic semiconductors and insulators are collected in Table 1. The solid state energy (SSE) scale is obtained by assessing an average EA (for a cation) or an average IP (for an anion) for each atom by using data from compounds having that specific atom as a constituent. For example, the SSE for Al (−2.1 eV) is the average EA for AlN, AlAs, and AlSb, whereas the SSE for P (−5.7 eV) is the average IP for AlP, GaP, and InP. This procedure gives rise to the SSE values summarized in Table 2.

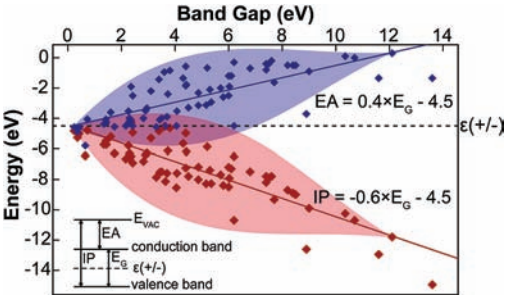


**Figure 1.** Electron affinity (EA, blue) and ionization potential (IP, red) versus energy band gap ($E_G$) for 69 binary closed-shell inorganic semiconductors and insulators. Regression lines for both EA and IP intersect at −4.5 eV (dashed line). The coefficients of determination ($R^2$) are 0.54 and 0.74 for the blue and red lines, respectively.

## RESULTS AND DISCUSSION

**Universal Hydrogen Energy Alignment.** A plot of electron affinity (EA) and ionization potential (IP) versus energy band gap ($E_G$) for 69 binary closed-shell inorganic compounds is shown in Figure 1. A regression analysis of the values for the 69 compounds listed in Table 1 reveals two surprising and illuminating trends. First, they have a common intercept of approximately 4.5 eV below the vacuum level. This intercept is shown as a dashed line in Figure 1. It corresponds to the hydrogen donor/acceptor ionization energy $\varepsilon(+/-)$[2] or, equivalently, to the standard hydrogen electrode (SHE) potential of electrochemistry as measured with respect to the vacuum level.[3] This correspondence suggests that $\varepsilon(+/-)$ constitutes an absolute

**Received:** May 21, 2011
**Published:** August 23, 2011

**Table 1. Properties of 69 Closed-Shell Binary Inorganic Compounds**

| compound | $E_G$ (eV) | EA (eV) | IP (eV) | SSE compound hardness (eV) | SSE1 ionicity (unitless) | SSE2 ionicity (unitless) | SSE3 ionicity (unitless) | Phillips ionicity (unitless)[70] | Pauling ionicity (unitless)[70] |
|---|---|---|---|---|---|---|---|---|---|
| **AlN** | 6.026[58] | −1.9[45] | −7.93 | 5.9 | 0.78 | 0.72 | 0.85 | 0.449 | 0.56 |
| **AlP** | 2.42[33] | −2.51[33] | −4.93 | 3.6 | 0.62 | 0.45 | 0.67 | 0.307 | 0.25 |
| **AlAs** | 2.36[36] | −1.91[35] | −4.27 | 2.9 | 0.54 | 0.33 | 0.58 | 0.274 | 0.27 |
| **AlSb** | 1.6[23] | −3.6[23] | −5.20 | 2.8 | 0.53 | 0.32 | 0.57 | 0.426 | 0.26 |
| **BaO** | 4.4[50] | −0.57[60] | −4.97 | 6.7 | 0.83 | 0.79 | 0.89 | | |
| **BaS** | 3.8[40] | −0.84[60] | −4.64 | 5.5 | 0.76 | 0.68 | 0.82 | | |
| **BaSe** | 3.6[56] | −0.95[60] | −4.55 | 5.7 | 0.77 | 0.70 | 0.84 | | |
| **BaTe** | 3.4[48] | −1.43[60] | −4.83 | 5.1 | 0.73 | 0.64 | 0.80 | | |
| **BN** | 6.2[47] | −4.5[23] | −10.7 | 3.5 | 0.61 | 0.43 | 0.66 | 0.256 | 0.42 |
| **CaO** | 6.8[47] | −0.7[60] | −7.50 | 6.0 | 0.79 | 0.74 | 0.86 | 0.913 | 0.97 |
| **CaS** | 4.6[44] | −1.85[60] | −6.45 | 4.8 | 0.71 | 0.61 | 0.78 | 0.902 | 0.81 |
| **CaSe** | 4.87[56] | −2.32[60] | −7.19 | 5.0 | 0.73 | 0.63 | 0.80 | 0.9 | 0.9 |
| **CaTe** | 4.07[56] | −3.53[60] | −7.60 | 4.4 | 0.68 | 0.56 | 0.75 | 0.894 | 0.88 |
| **$CaF_2$** | 12.1[47] | 0.3[53] | −11.8 | 10.5 | 0.97 | 0.97 | 0.99 | | |
| **CdO** | 2.16[39] | −4.5[31] | −6.66 | 3.1 | 0.57 | 0.38 | 0.62 | 0.785 | 0.85 |
| **CdS** | 2.42[33] | −4.5[33] | −6.92 | 1.9 | 0.41 | 0.17 | 0.42 | 0.685 | 0.59 |
| **CdSe** | 1.74[33] | −4.56[33] | −6.30 | 2.1 | 0.45 | 0.21 | 0.46 | 0.699 | 0.58 |
| **CdTe** | 1.44[33] | −4.28[33] | −5.72 | 1.5 | 0.36 | 0.12 | 0.35 | 0.675 | 0.52 |
| **CsI** | 6.2[52] | −0.3[52] | −6.50 | 6.7 | 0.83 | 0.79 | 0.89 | | |
| **GaN** | 3.43[58] | −4.1[45] | −7.53 | 4.1 | 0.66 | 0.51 | 0.72 | 0.5 | 0.55 |
| **GaP** | 2.26[23] | −4.3[33] | −6.56 | 1.8 | 0.39 | 0.16 | 0.40 | 0.374 | 0.27 |
| **GaAs** | 1.42[57] | −4.07[33] | −5.49 | 1.1 | 0.27 | 0.06 | 0.25 | 0.31 | 0.26 |
| **GaSb** | 0.726[33] | −4.06[33] | −4.79 | 1.0 | 0.25 | 0.05 | 0.23 | 0.261 | 0.26 |
| **InN** | 0.65[37] | −5.8[46] | −6.45 | 3.4 | 0.59 | 0.41 | 0.64 | 0.578 | 0.5 |
| **InP** | 1.344[33] | −4.38[33] | −5.72 | 1.1 | 0.27 | 0.07 | 0.26 | 0.421 | 0.26 |
| **InAs** | 0.36[33] | −4.9[33] | −5.26 | 0.4 | 0.11 | 0.01 | 0.09 | 0.357 | 0.26 |
| **InSb** | 0.235[25] | −4.59[23] | −4.83 | 0.3 | 0.09 | 0.01 | 0.07 | 0.321 | 0.25 |
| **KF** | 10.7[52] | 0[52] | −10.7 | 11.5 | 1.00 | 1.00 | 1.00 | 0.955 | 0.99 |
| **KCl** | 8.4[52] | −0.5[52] | −8.90 | 8.7 | 0.91 | 0.91 | 0.95 | 0.953 | 0.95 |
| **KBr** | 7.4[52] | −0.8[52] | −8.20 | 7.3 | 0.86 | 0.83 | 0.91 | 0.952 | 0.91 |
| **KI** | 6[52] | −1.2[52] | −7.20 | 6.4 | 0.81 | 0.77 | 0.88 | 0.95 | 0.92 |
| **LiF** | 13.6[52] | −1.35[30] | −14.95 | 11.3 | 0.99 | 0.99 | 1.00 | 0.915 | 0.98 |
| **LiBr** | 7.6[52] | −0.2[52] | −7.80 | 7.1 | 0.85 | 0.82 | 0.91 | 0.899 | 0.93 |
| **MgO** | 7.7[22] | −1.63[38] | −9.33 | 4.5 | 0.70 | 0.58 | 0.76 | 0.841 | 0.88 |
| **MgS** | 4.87[22] | −3.15[60] | −8.02 | 3.3 | 0.58 | 0.40 | 0.63 | 0.786 | 0.78 |
| **MgSe** | 4.05[22] | −4.5[60] | −8.55 | 3.5 | 0.61 | 0.43 | 0.66 | 0.79 | 0.77 |
| **NaF** | 11.6[52] | −1.35[30] | −12.95 | 11.3 | 0.99 | 0.99 | 1.00 | 0.946 | 0.98 |
| **NaCl** | 8.5[52] | −0.5[52] | −9.00 | 8.1 | 0.89 | 0.88 | 0.94 | 0.935 | 0.94 |
| **NaBr** | 7.5[52] | −0.4[52] | −7.90 | 7.1 | 0.85 | 0.82 | 0.91 | 0.934 | 0.93 |
| **PbS** | 0.4[47] | −4.6[42] | −5.00 | 1.80 | 0.39 | 0.18 | 0.43 | | |
| **RbF** | 10.35[52] | 0.1[52] | −10.25 | 11.6 | 1.00 | 1.00 | 1.00 | 0.96 | 0.99 |
| **RbCl** | 8.2[52] | −0.5[52] | −8.70 | 8.4 | 0.90 | 0.89 | 0.94 | 0.955 | 0.95 |
| **RbBr** | 7.4[52] | −0.4[52] | −7.80 | 7.4 | 0.86 | 0.84 | 0.92 | 0.957 | 0.94 |
| **RbI** | 6.1[52] | −1.2[52] | −7.30 | 6.5 | 0.82 | 0.78 | 0.88 | 0.951 | 0.92 |
| **SiC** | 2.36[45] | −4.0[26] | −6.36 | 4.1 | 0.66 | 0.52 | 0.72 | 0.177 | 0.11 |
| **$Si_3N_4$** | 5.3[55] | −2.1[55] | −7.42 | 5.7 | 0.77 | 0.85 | 0.92 | | |
| **$SnS_2$** | 2.31[65] | −4.2[65] | −6.64 | 2.0 | 0.42 | 0.18 | 0.43 | | |
| **SrO** | 5.2[47] | −0.67[60] | −5.87 | 6.1 | 0.80 | 0.74 | 0.86 | 0.926 | 0.93 |
| **SrS** | 4.3[32] | −1.35[60] | −5.65 | 4.9 | 0.72 | 0.61 | 0.78 | 0.914 | 0.91 |
| **SrSe** | 4.42[56] | −1.77[60] | −6.19 | 5.1 | 0.73 | 0.64 | 0.80 | 0.917 | 0.8 |
| **SrTe** | 3.73[56] | −2.4[60] | −6.13 | 4.5 | 0.69 | 0.57 | 0.75 | 0.903 | 0.75 |
| **ZnO** | 3.3[61] | −4.57[61] | −7.87 | 3.6 | 0.62 | 0.45 | 0.67 | 0.616 | 0.8 |
| **ZnS** | 3.7[47] | −3.9[22] | −7.60 | 2.4 | 0.48 | 0.25 | 0.50 | 0.623 | 0.59 |


dx.doi.org/10.1021/ja204670s |J. Am. Chem. Soc. 2011, 133, 16852–16860

**Table 1. Continued**

| compound | $E_G$ (eV) | EA (eV) | IP (eV) | SSE compound hardness (eV) | SSE1 ionicity (unitless) | SSE2 ionicity (unitless) | SSE3 ionicity (unitless) | Phillips ionicity (unitless)[70] | Pauling ionicity (unitless)[70] |
|---|---|---|---|---|---|---|---|---|---|
| **ZnSe** | 2.82[33] | −4[33] | −6.82 | 2.6 | 0.51 | 0.29 | 0.54 | 0.676 | 0.57 |
| **ZnTe** | 2.26[33] | −3.53[33] | −5.79 | 2.0 | 0.43 | 0.19 | 0.44 | 0.546 | 0.53 |
| **$HfO_2$** | 5.7[24] | −2[49] | −7.7 | 5.6 | 0.77 | 0.70 | 0.84 | | |
| **$ZrO_2$** | 5.8[55] | −2.6[61] | −8.4 | 5.0 | 0.73 | 0.64 | 0.80 | | |
| **$SiO_2$** | 9.0[57] | −0.9[57] | −9.9 | 5.3 | 0.75 | 0.67 | 0.82 | | |
| **$GeO_2$** | 5.35[47] | −2.93[63] | −8.28 | 4.7 | 0.71 | 0.60 | 0.78 | | |
| **$SnO_2$** | 3.64[47] | −4.5[50] | −8.14 | 3.2 | 0.58 | 0.39 | 0.63 | | |
| **$MoO_3$** | 3.1[54] | −2.2[34] | −5.3 | 5.4 | 0.76 | 0.68 | 0.83 | | |
| **$WO_3$** | 2.95[54] | −3.33[62] | −6.28 | 4.3 | 0.68 | 0.55 | 0.74 | | |
| **$Al_2O_3$** | 8.7[64] | −3.71[29] | −12.42 | 5.5 | 0.76 | 0.69 | 0.83 | | |
| **$Ga_2O_3$** | 4.8[47] | −3.2[59] | −8.0 | 3.7 | 0.62 | 0.46 | 0.68 | | |
| **$In_2O_3$** | 2.9[7] | −3.5[41] | −6.4 | 3.0 | 0.56 | 0.35 | 0.60 | | |
| **$V_2O_5$** | 2.3[28] | −4[66] | −6.3 | 3.6 | 0.62 | 0.45 | 0.67 | | |
| **$La_2O_3$** | 6[51] | −2.5[51] | −8.5 | 5.1 | 0.74 | 0.65 | 0.81 | | |
| **$Ta_2O_5$** | 4.5[64] | −3.2[43] | −7.7 | 4.4 | 0.69 | 0.57 | 0.75 | | |
| **$TiO_2$** | 3.05[64] | −4.2[27] | −7.25 | 3.4 | 0.60 | 0.42 | 0.65 | | |

energy reference. This assertion is supported by the fact that the majority of EA and IP values included in Figure 1 are found above or below $\varepsilon(+/-)$, respectively. Electronic charge transfer will occur from a higher energy state to a lower energy state, so the conduction and valence bands, cf., the insert in Figure 1, are associated with cationic and anionic character, respectively. Second, the slopes of both regression lines have a value of approximately 0.5, suggesting that the band gap of an inorganic semiconductor or insulator is on average centered at $\varepsilon(+/-)$. This result also implies that EA and IP for any semiconductor or insulator may be estimated to first order by simply knowing $E_G$ and recognizing that $\varepsilon(+/-)$ serves as an absolute energy reference for positioning the center of the gap, as shown in the insert of Figure 1.

**Solid State Energy Scale.** The SSE scale, arranged in descending energy order, is shown in Figure 2. The values were derived according to the procedure described in the Methods section. The calculated SSE values are specified as negative quantities, since they are referenced to the vacuum level.[4] Note that the energy $\varepsilon(+/-)$ acts as a demarcation between *typical* cationic and anionic behavior.

That is, an atom with a SSE more negative than $\varepsilon(+/-)$ tends to be an anion, whereas an atom with a SSE less negative than $\varepsilon(+/-)$ tends to be a cation. This tendency arises simply from energetic considerations; electronic charge transfer occurs from a higher frontier orbital energy state to a lower frontier orbital energy state.

Frontier orbital energy positioning with respect to $\varepsilon(+/-)$, however, is not a rigid guide to predicting cation and anion behavior in a compound. Rather, energetic considerations inherent in relevant SSE positioning of each atom in Figure 2 are more important. For example, although Te may be classified as an anion on the basis of its SSE being more negative than $\varepsilon(+/-)$, cf. Figure 2, it actually functions as a cation in the compound $TeO_3$. This behavior occurs because, using Figure 2 as a guide, the SSE of O is more negative than that of Te. In $TeO_3$, electronic charge transfers from Te to O. From these considerations, oxides may be classified as basic, acidic, or amphoteric in the following way: a cation with a SSE less negative than $\varepsilon(+/-)$ tends to form a basic oxide, a cation with a SSE more negative than $\varepsilon(+/-)$ tends to form an acidic oxide, and a cation with a SSE similar to $\varepsilon(+/-)$ tends to form an amphoteric oxide.[5]

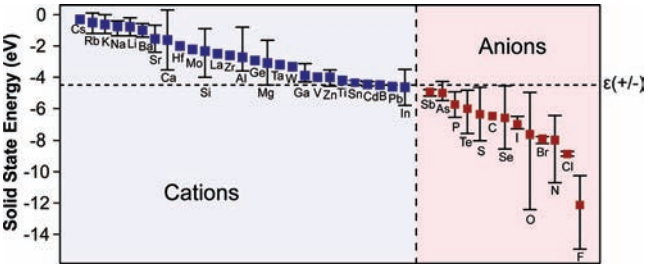


**Figure 2.** Solid state energy (SSE) values for 40 elements arranged in descending energy order. SSE is assessed as an average EA (for a cation, shown in blue) or an average IP (for an anion, shown in red) for binary compounds having the atom under consideration as a constituent. Error bars correspond to maximum and minimum values from the available data. The dashed horizontal line at 4.5 eV corresponds to the hydrogen donor/acceptor ionization energy $[\varepsilon(+/-)]$ or, equivalently, to the standard hydrogen electrode (SHE) potential of electrochemistry as measured with respect to the vacuum level.

The SSE scale has numerous practical applications. It can be used to directly assess optical band gaps and anticipate the character of valence and conduction bands. For example, a simple difference between the SSEs of In (−4.6 eV) and O (−7.6 eV) provides an estimate of the band gap of $In_2O_3$ ($E_G$ = 3.2 eV), which compares well to the measured value of 2.9 eV.[6] How will this gap change in more complex materials such as $CaIn_2O_4$? Comparison of the In and O SSE values with Ca (−1.6 eV) reveals that the character of the bottom of the conduction band in $CaIn_2O_4$ should be dominated by In. The dilution of In by Ca relative to binary $In_2O_3$, however, will decrease the dispersion of the In conduction band and increase the band gap. So, it is not surprising that the reported band gap of $CaIn_2O_4$, 3.9 eV,[7] is greater than that of $In_2O_3$. Correspondingly, the SSEs of In (−4.6 eV) and S (−6.4 eV) give an estimated band gap for $In_2S_3$ of 1.8 eV, which compares well to the measured value of 2.1 eV.[8] In the ternary material $MgIn_2S_4$, the

**Table 2. Atomic Properties for 40 Elements; IP is the Ionization Energy, EA is the Electron Affinity and $RE^{SSE}$ is the Solid State Renormalization Energy in Going from the Gas to Solid Phase**

| element | atomic number | SSE (eV) | IP (eV)[67] | EA (eV)[68] | Mulliken EN (eV)[69] | $RE^{SSE}$ (eV) |
|---|---|---|---|---|---|---|
| Li | 3 | −0.8 | 5.39 | 0.62 | 3.01 | 5.0 |
| B | 5 | −4.5 | 8.30 | 0.28 | 4.29 | 3.8 |
| C | 6 | −6.4 | 11.26 | 1.26 | 6.27 | 4.8 |
| N | 7 | −8.0 | 14.53 | −0.07 | 7.3 | 6.5 |
| O | 8 | −7.6 | 13.62 | 1.46 | 7.54 | 5.7 |
| F | 9 | −12.1 | 17.42 | 3.40 | 10.41 | 5.7 |
| Na | 11 | −0.8 | 5.14 | 0.55 | 2.85 | 4.6 |
| Mg | 12 | −3.1 | 7.65 | −0.40 | 3.75 | 4.9 |
| Al | 13 | −2.1 | 5.99 | 0.44 | 3.23 | 3.3 |
| Si | 14 | −2.3 | 8.15 | 1.39 | 4.77 | 5.8 |
| P | 15 | −5.7 | 10.49 | 0.75 | 5.62 | 4.8 |
| S | 16 | −6.4 | 10.36 | 2.08 | 6.22 | 4.0 |
| Cl | 17 | −8.9 | 12.97 | 3.62 | 8.3 | 3.6 |
| K | 19 | −0.6 | 4.34 | 0.50 | 2.42 | 3.7 |
| Ca | 20 | −1.6 | 6.11 | −0.30 | 2.2 | 4.5 |
| Ti | 22 | −4.2 | 6.82 | 0.08 | 3.45 | 3.0 |
| V | 23 | −4.0 | 6.74 | 0.53 | 3.6 | 2.7 |
| Zn | 30 | −4.0 | 9.39 | −0.60 | 4.45 | 5.4 |
| Ga | 31 | −3.9 | 6.00 | 0.30 | 3.2 | 2.1 |
| Ge | 32 | −2.9 | 7.90 | 1.20 | 4.6 | 5.0 |
| As | 33 | −5.0 | 9.82 | 0.81 | 5.3 | 4.8 |
| Se | 34 | −6.6 | 9.75 | 2.02 | 5.89 | 3.2 |
| Br | 35 | −7.9 | 11.81 | 3.37 | 7.59 | 3.9 |
| Rb | 37 | −0.5 | 4.18 | 0.49 | 2.34 | 3.7 |
| Sr | 38 | −1.6 | 5.69 | −0.30 | 2 | 4.2 |
| Zr | 40 | −2.6 | 6.84 | 0.43 | 3.64 | 4.2 |
| Mo | 42 | −2.2 | 7.10 | 0.75 | 3.9 | 4.9 |
| Cd | 48 | −4.5 | 8.99 | −0.70 | 4.33 | 4.5 |
| In | 49 | −4.6 | 5.79 | 0.30 | 3.1 | 1.2 |
| Sn | 50 | −4.4 | 7.34 | 1.20 | 4.3 | 3.0 |
| Sb | 51 | −4.9 | 8.64 | 1.07 | 4.85 | 3.7 |
| Te | 52 | −6.0 | 9.01 | 1.97 | 5.49 | 3.0 |
| I | 53 | −7.0 | 10.45 | 3.06 | 6.76 | 3.5 |
| Cs | 55 | −0.3 | 3.89 | 0.47 | 2.18 | 3.5 |
| Ba | 56 | −1.0 | 5.21 | −0.30 | 2.4 | 4.3 |
| La | 57 | −2.5 | 5.58 | 0.50 | 3.1 | 3.1 |
| Hf | 72 | −2.0 | 7.00 | 0.00 | 3.8 | 5.0 |
| Ta | 73 | −3.2 | 7.89 | 0.32 | 4.11 | 4.3 |
| W | 74 | −3.3 | 7.98 | 0.82 | 4.4 | 4.7 |
| Pb | 82 | −4.6 | 7.42 | 0.36 | 3.9 | 2.8 |

SSE of Mg (−3.1 eV) is above that of In. The bottom of the conduction band will then be dominated by In character with a small increase in band gap, 2.3 eV,[9] relative to that of $In_2S_3$. Hence, for complex compositions SSE values are simply stacked, and the gap is derived by considering the energy difference between the most negative cation SSE and the least negative anion SSE.

**Electronegativity.** SSE is an alternative approach to electronegativity (EN). Comparing SSE values to Pauling[10] and Mulliken[11] electronegativities[12] for 40 elements (Figure 3), it is clear that SSE captures the periodic trends of electronegativity.

An advantage of SSE and Mulliken electronegativity, compared to Pauling electronegativity, is that they both have units of energy. When comparing SSE and Mulliken electronegativities on an absolute energy scale, (part a of Figure 4, Table 2), as opposed to the dimensionless Pauling scale (Figure 3), it is clear from part b of Figure 4 that they are correlated (correlation coefficient = 0.88).

The correlation is high for more negative SSEs and lower for less negative SSEs (parts a and b of Figure 4). There is also a persistent discrepancy between SSE and Mulliken electronegativity as evident from the large regression intercept energy of 1.8 eV (part b of Figure 4). For example, the SSE magnitude for Cs is 0.3 eV compared with the Mulliken electronegativity of 2.18 eV. To discover the origin of this energy offset, it is necessary to review the formulation of Mulliken electronegativity.

Mulliken electronegativity[11] of an atom X (Table 2, column 6) is defined as

$$EN^{Mulliken}(X) = \frac{I(X) + A(X)}{2}(eV) \quad (1)$$

where $I(X)$ and $A(X)$ are the ionization energy (Table 2, column 4) and the electron affinity (Table 2, column 5) respectively of atom X in the *gas phase*.[13] Mulliken argued from physical principles for the viability of taking an average of I and A as an absolute energy reference of electronegativity. Note, however, for the 40 elements listed in Table 2, that $I$(average) = 8.2 eV and $A$(average) = 0.8 eV. Thus, inclusion of A only contributes ~10% to estimating electronegativity. The addition of A does allow Mulliken to divide *gas phase* quantities by 2. We contend that this division by 2 is essentially an energy renormalization procedure, allowing gas phase energies to be renormalized to an energy scale more appropriate for the solid state. In support of this contention, notice that for the 40 elements included in Table 2, $EN^{MULLIKEN}$(average) = 4.5 eV and SSE(average) = 4.1 eV. Although Mulliken had no way of knowing it at the time, his average electronegativity would have been closer to SSE(average), that is, 4.1 eV instead of 4.5 eV, if he simply ignored A (and retained division by 2) in his definition of electronegativity. From the SSE perspective, electronegativity involves positioning the relative energies of frontier orbitals. Thus, it would have been better if Mulliken had defined electronegativity as simply equal to the ionization energy, $I$.[14] Recognize, however, that this formulation of electronegativity corresponds to a *gas phase* energy scale.

Instead of simple division by 2, energy differences between the gas phase and the solid state can be modeled by introducing a solid state renormalization energy for an atom X, defined as

$$RE^{SSE}(X) = I(X) + SSE(X)(eV) \quad (2)$$

$RE^{SSE}(X)$ is a positive quantity, because $I(X)$, also a positive quantity, is always larger in magnitude than the negative quantity SSE(X). $RE^{SSE}(X)$ is tabulated in Table 2 (column 7). For the 40 elements included in Table 2, $RE^{SSE}$(average) = 4.1 eV. Although this value of $RE^{SSE}$(average) supports Mulliken's division by 2 as an appropriate way to renormalize between gas phase and solid state energy scales in an average sense, the high degree of $RE^{SSE}$ variability (the range of $RE^{SSE}$ in Figure 5 is 6.1 eV) highlights the limitations of this approach.

Specifically, the poor agreement between SSE and $EN^{MULLIKEN}$ for less negative SSEs observed in part a of Figure 4 is a consequence of the inadequacy of accounting for $RE^{SSE}$ by renormalizing energy with a simple division by 2. This leads to the large regression line intercept energy of 1.8 eV in part b of Figure 4.

The relationship between SSE and Pauling electronegativity can be established by plotting Pauling electronegativity vs the square root of SSE and then performing a least-squares fit (part a of Figure 6) to give

$$SSE(Pauling) = 1.05\sqrt{|SSE|} - 0.12(Pauling\ units) \quad (3)$$

Atomic values for Pauling electronegativity and SSE (Pauling) are summarized in Table 3, columns 3 and 4, respectively.

This procedure for converting to Pauling units was developed by Bratsch,[15] and it is preferred because it is dimensionally correct (the Pauling scale has the dimension of the square root of energy). The SSE−Pauling electronegativity correlation is quite good, as evident from the near unity slope and near-zero intercept of the regression line as well as the correlation coefficient of 0.83.

For comparison, Mulliken electronegativity is also converted to Pauling units using the approach of Bratsch, yielding (part b of Figure 6)

$$EN^{Mulliken}(Pauling) = 1.73\sqrt{EN^{Mulliken}} - 1.71(Pauling\ units) \quad (4)$$

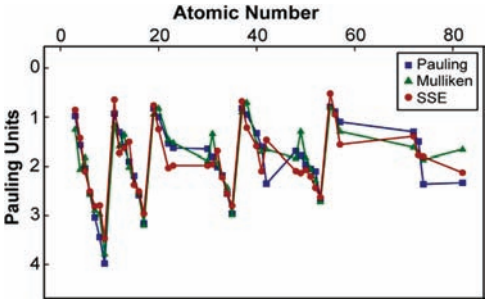


**Figure 3.** Atomic solid state energy (SSE), Pauling electronegativity, and Mulliken electronegativity versus atomic number for 40 elements plotted in Pauling units.

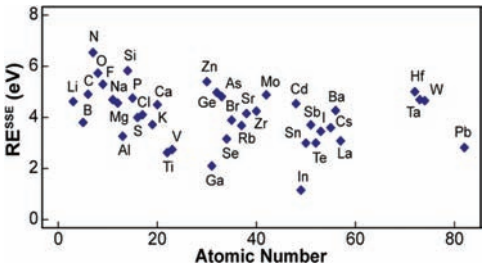


**Figure 5.** Solid state renormalization energy in going from the gas phase to the solid state ($RE^{SSE}$) versus atomic number for 40 elements.

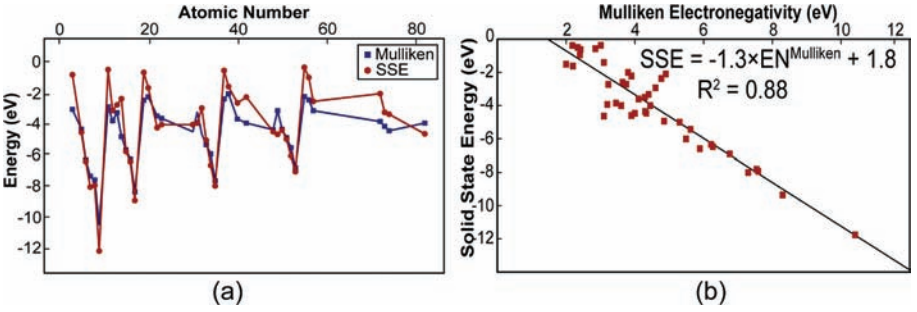


**Figure 4.** a) Atomic solid state energy (SSE) versus Mulliken electronegativity ($EN^{Mulliken}$) for 40 elements. b) Regression plot of atomic SSE versus Mulliken electronegativity.

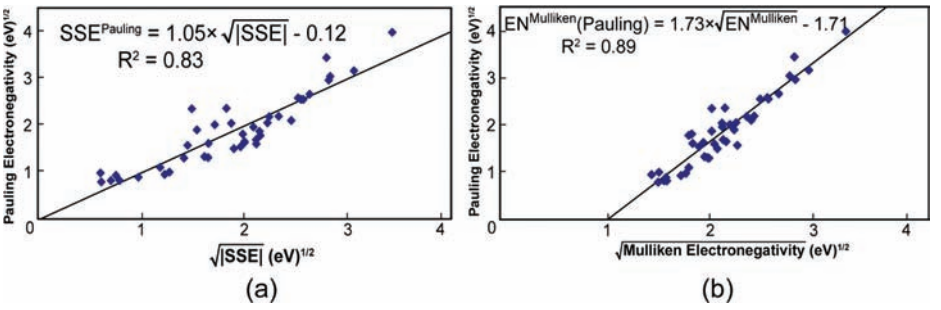


**Figure 6.** Pauling electronegativity versus the square root of a) the solid state energy (SSE) and b) the Mulliken electronegativity.

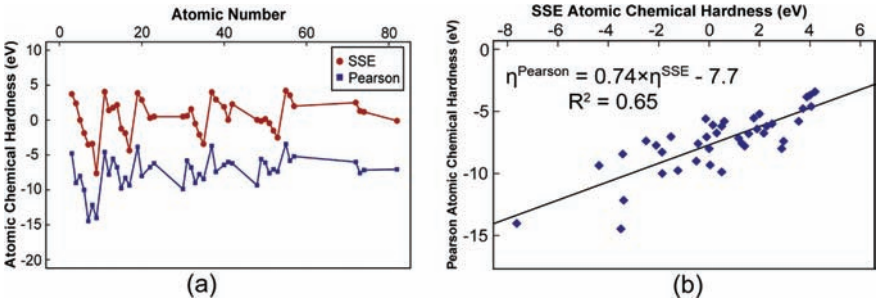


**Figure 7.** a) Solid state energy chemical hardness ($\eta^{SSE}(X)$) and Pearson chemical hardness ($\eta^{Pearson}(X)$) for an atom X versus atomic number. b) Regression plot between Pearson atomic chemical hardness and SSE atomic chemical hardness.

The Mulliken−Pauling electronegativity correlation is similar from the perspective of the 0.89 value of the regression line correlation coefficient. However, the regression line slope of 1.73 and intercept of 1.71 are further evidence for the existence of a gas phase energy offset in the Mulliken formulation of electronegativity.

The SSE perspective provides a new, quantitative basis for assessing, conceptualizing, and implementing electronegativity. According to Pauling, electronegativity is "the power of an atom in a molecule to attract electrons to itself".[16] Here, the "power of attraction" simply arises from the relative SSEs of the elements constituting the compound.

**Chemical Hardness.** Chemical hardness can also be considered within the SSE framework. Chemical hardness originated as a classification scheme for predicting acid−base reactivity in solution.[17] The principles of chemical hardness, however, can also be employed to classify elements as acids and bases. Hard acids and bases tend to be small and nonpolarizable, readily bonding with one another to form ionic bonds. In contrast, soft acids and bases tend to be large and polarizable, readily bonding with each other to form covalent bonds. Note that atoms in Figure 2 with more or less negative SSEs are hard acids or hard bases, respectively, while atoms with SSEs positioned slightly above and below $\varepsilon(+/-)$ are soft acids and bases, respectively. In the solid state, chemical hardness is quantitatively defined as being equal to $E_G$.[18] From these considerations, the SSE chemical hardness, $\eta$, of an *atom* X is defined as

$$\eta^{SSE}(X) = SSE(X) - \varepsilon(+/-)\,(eV) \quad (5)$$

It then follows that the SSE chemical hardness of a binary AB compound is formulated as

$$\eta^{SSE}(AB) = SSE(A) - SSE(B)\,(eV) \quad (6)$$

For comparison, the conventional Pearson chemical hardness[17,18] of an *atom* X is defined as

$$\eta^{Pearson}(X) = I(X) - A(X)\,(eV) \quad (7)$$

where $I$ and $A$ are the ionization potential and the electron affinity respectively of atom X in the *gas phase*. Because both types of hardness are expressed in eV units, they may be directly compared by plotting Pearson hardness as a negative quantity on the SSE scale (part a of Figure 7). The correlation between $\eta^{SSE}(X)$ and $\eta^{Pearson}(X)$ is evident in part a of Figure 7, although they are offset in energy.

A regression line fit to a plot of $\eta^{SSE}(X)$ versus $\eta^{Pearson}(X)$ yields a correlation coefficient of 0.65 and an offset energy of 7.7 eV (part b of Figure 7). 4.5 eV of this 7.7 eV offset is accounted for by redefining $\varepsilon(+/-)$ as the origin of the SSE chemical hardness axis. The remaining 3.2 eV offset is attributed to $RE^{SSE}$, as discussed previously with respect to Mulliken electronegativity. Note that this 3.2 eV offset is approximately twice the offset energy obtained from the graph in part b of Figure 4. This is not a coincidence. $EN^{MULLIKEN}$ is defined as $[I(X) + A(X)]/2$, whereas $\eta^{Pearson}$ is defined as $[I(X) - A(X)]$, so a factor of 2 difference between regression line intercept energies is expected. Importantly, energy differences between SSE and $EN^{MULLIKEN}$ and $\eta^{Pearson}$ are a consequence of the fact that SSE is a solid state scale whereas $EN^{MULLIKEN}$ and $\eta^{Pearson}$ are both gas phase scales.

For a compound, the SSE approach allows one to compare a *predicted* chemical hardness ($SSE_A - SSE_B$) and an *actual* chemical hardness ($E_G$). Such a comparison for 69 binary inorganic semiconductors and insulators (Figure 8) yields a regression line with a slope near unity, an intercept near zero, and a correlation coefficient of 0.82, demonstrating the viability of SSE band gap estimation.

**Table 3. Atomic Properties for 40 Elements; Columns 3, 4, and 5 Refer to Pauling Electronegativity, Solid State Energy, and Mulliken Electronegativity Expressed in Pauling Units; Columns 6 and 7 are SSE Atomic Hardness Calculated Using eq 6 and Pearson Atomic Hardness**

| element | atomic number | Pauling EN (Pauling units)[12] | SSE (Pauling units) | Mulliken EN (Pauling units) | SSE atomic hardness (eV) | Pearson hardness (eV)[17,18] |
|---|---|---|---|---|---|---|
| Li | 3 | 0.98 | 0.80 | 1.29 | 3.73 | 4.78 |
| B | 5 | 2.04 | 2.11 | 1.87 | 0.00 | 8 |
| C | 6 | 2.55 | 2.53 | 2.62 | −1.98 | 10 |
| N | 7 | 3.04 | 2.85 | 2.96 | −3.50 | 14.46 |
| O | 8 | 3.44 | 2.78 | 3.04 | −3.14 | 12.16 |
| F | 9 | 3.98 | 3.54 | 3.87 | −7.63 | 14.02 |
| Na | 11 | 0.93 | 0.79 | 1.21 | 3.75 | 4.6 |
| Mg | 12 | 1.31 | 1.73 | 1.64 | 1.41 | 7.8 |
| Al | 13 | 1.61 | 1.61 | 1.40 | 1.77 | 5.54 |
| Si | 14 | 1.9 | 1.48 | 2.07 | 2.17 | 6.76 |
| P | 15 | 2.19 | 2.40 | 2.39 | −1.24 | 9.76 |
| S | 16 | 2.58 | 2.53 | 2.60 | −1.87 | 8.28 |
| Cl | 17 | 3.16 | 3.01 | 3.27 | −4.37 | 9.36 |
| K | 19 | 0.82 | 0.71 | 0.98 | 3.88 | 3.84 |
| Ca | 20 | 1 | 1.22 | 0.86 | 2.88 | 8 |
| Ti | 22 | 1.54 | 2.03 | 1.50 | 0.30 | 6.74 |
| V | 23 | 1.63 | 1.98 | 1.57 | 0.50 | 6.2 |
| Zn | 30 | 1.65 | 1.98 | 1.94 | 0.50 | 9.88 |
| Ga | 31 | 1.81 | 1.97 | 1.38 | 0.55 | 5.8 |
| Ge | 32 | 2.01 | 1.68 | 2.00 | 1.57 | 6.8 |
| As | 33 | 2.18 | 2.23 | 2.27 | −0.51 | 9 |
| Se | 34 | 2.55 | 2.58 | 2.49 | −2.10 | 7.74 |
| Br | 35 | 2.96 | 2.84 | 3.06 | −3.43 | 8.44 |
| Rb | 37 | 0.82 | 0.62 | 0.94 | 4.00 | 3.7 |
| Sr | 38 | 0.95 | 1.19 | 0.74 | 2.95 | 7.4 |
| Zr | 40 | 1.33 | 1.57 | 1.59 | 1.90 | 6.42 |
| Mo | 42 | 2.35 | 1.44 | 1.71 | 2.28 | 6.2 |
| Cd | 48 | 1.69 | 2.10 | 1.89 | 0.04 | 9.32 |
| In | 49 | 1.78 | 2.14 | 1.34 | −0.13 | 5.6 |
| Sn | 50 | 1.96 | 2.07 | 1.88 | 0.15 | 6.1 |
| Sb | 51 | 2.05 | 2.21 | 2.10 | −0.44 | 7.6 |
| Te | 52 | 2.1 | 2.45 | 2.34 | −1.51 | 7.04 |
| I | 53 | 2.66 | 2.66 | 2.79 | −2.50 | 7.38 |
| Cs | 55 | 0.79 | 0.46 | 0.84 | 4.20 | 3.42 |
| Ba | 56 | 0.89 | 0.93 | 0.97 | 3.50 | 5.8 |
| La | 57 | 1.1 | 1.54 | 1.34 | 2.00 | 5.2 |
| Hf | 72 | 1.3 | 1.36 | 1.66 | 2.50 | 6 |
| Ta | 73 | 1.5 | 1.76 | 1.80 | 1.30 | 7.58 |
| W | 74 | 2.36 | 1.80 | 1.92 | 1.17 | 7.16 |
| Pb | 82 | 2.33 | 2.13 | 1.71 | −0.10 | 7.06 |

**Ionicity.** The SSE plot shown in Figure 2 leads to a fresh approach for qualitatively assessing covalency and ionicity. In the compound InSb, the SSEs for In (−4.6 eV) and Sb (−4.9 eV) are energetically very similar, because they are both positioned near $\varepsilon(+/-)$. Because their frontier orbital energies are similar, a high degree of electron sharing and covalent bonding are expected. In LiF, however, the shallow energy of the Li frontier orbital (SSE = −0.8 eV) in conjunction with the extraordinarily large energy depth of F (SSE = −12.1 eV) leads to a significant charge transfer from Li to F, characteristic of a strongly ionic bond. In short, binary compounds with both SSEs near $\varepsilon(+/-)$ are expected to be covalent, whereas compounds with both SSEs remote from $\varepsilon(+/-)$ are expected to be ionic.

The SSE scale provides a new method for determining ionicity, $f_i$, which is an estimate of the fractional ionic character of a chemical bond.[19] It is defined to be equal to one for a purely ionic bond and zero for a purely covalent bond. Our previous consideration of Figure 2 indicates that covalent behavior involves combining atoms with similar SSEs and those near $\varepsilon(+/-)$, whereas ionic bonding is maximized by choosing atoms with distinctly different SSEs and those far above and below $\varepsilon(+/-)$. Thus, $\varepsilon(+/-)$ can be taken to be a measure of

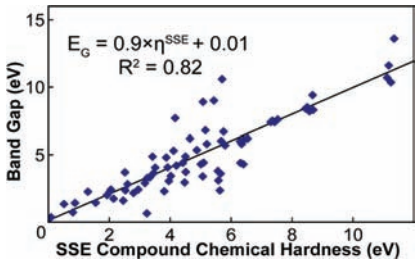


**Figure 8.** Energy band gap versus solid state energy chemical hardness of 69 binary closed-shell inorganic semiconductors and insulators.

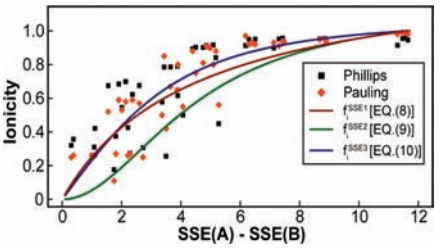


**Figure 9.** Ionicity ($f_i$) versus the difference in atomic solid state energy [SSE($A$) − SSE($B$)] in 46 AB compounds. Diamonds and squares correspond to Pauling and Phillips ionicities, respectively. Solid curves correspond to SSE1 (eq 8, red), SSE2 (eq 9, green), and SSE3 (eq 10, blue).

covalent bonding, whereas a SSE deviation from $\varepsilon(+/-)$ is an indicator of ionic bonding. We consider three quantitative SSE ionicity models for a compound AB by using $\varepsilon(+/-)$ and SSE(A) − SSE(B) respectively as estimates of covalent and ionic character:

$$f_i^{SSE1}(AB) = \frac{1.4[SSE(A) - SSE(B)]}{SSE(A) - SSE(B) + \varepsilon(+/-)}(\text{unitless}) \quad (8)$$

$$f_i^{SSE2}(AB) = \frac{1.16[SSE(A) - SSE(B)]^2}{[SSE(A) - SSE(B)]^2 + [\varepsilon(+/-)]^2}(\text{unitless}) \quad (9)$$

and

$$f_i^{SSE3}(AB) = \sqrt{f_i^{SSE2}(AB)}(\text{unitless}) \quad (10)$$

In eq 8, $f_i^{SSE1}$ is a SSE ionicity that is derived by simply adding covalent and ionic estimates as real numbers. In eq 9, the calculation of $f_i^{SSE2}$ follows the approach advocated by Phillips,[19] where covalent and ionic terms are combined as real and imaginary numbers, respectively. In eq 10, we follow the procedure of Harrison,[20] where $f_i^{SSE3}$is simply the square root of $f_i^{SSE2}$. The constants, 1.4 and 1.16, in eqs 8 and 9, respectively, are factors for normalizing the maximum difference between SSE($A$) and SSE($B$) to unit ionicity. This difference is encountered in LiF, that is, $f_i^{SSE1}$(LiF) = $f_i^{SSE2}$(LiF) = 1 for SSE(Li) − SSE(F) = 11.3 eV. The three derived ionicities are plotted as a function of the difference SSE($A$) − SSE($B$) for 46 binary compounds in Figure 9; for comparison, Phillips and Pauling values are also included.

The ionicities derived from the SSEs track those of Phillips and Pauling with the $f_i^{SSE3}$ curve perhaps offering the best fit. The large variability in the data, however, precludes drawing a final conclusion with respect to the optimal approach for estimating $f_i$ with SSEs. The ionicities $f_i^{SSE1}$, $f_i^{SSE2}$, and $f_i^{SSE3}$ as well as those of Phillips and Pauling are summarized in Table 1 (columns 6−10).

The SSE for each atom does not constitute a definitive value due to the variability in the data, reflected by the error bars depicted in Figure 2. Two sources of variability contribute to the magnitude of the error bars. These bars simply represent the full range of EA and IP values reported for each atom. The first source of variability is experimental uncertainty associated with empirical estimation of EA or IP. Often, IP is estimated via photoemission and then EA is found by subtraction of $E_G$. Determination of IP is usually the greatest source of error. Surface dipoles, surface band bending, and related effects can influence experimental results;[21] careful sample preparation and experimental techniques can limit uncertainties. The second source of variability is more interesting. If experimental error were limited and values of EA and IP were precisely determined, a range of EA and IP values would still be expected. In this case, subtle chemical bonding trends related to covalency and ionicity would be revealed.

## CONCLUSIONS

The SSE scale enables a novel perspective for unifying foundational chemical concepts across the solid state, solution, and gas phases. This scale provides a simple and intuitive understanding of concepts such as electronegativity, chemical hardness, and ionicity based on the relative positioning of the constituent atoms in a compound on an absolute energy scale. Because the SSE scale is empirical, the atomic values reported herein are subject to refinement as new and more accurate EA and IP data become available. Such data will lead to SSE estimates with improved reliability and, significantly, a robust accounting of SSE variability. Hence, the SSE scale provides a unique way to predict and quantitatively assess the electronic structure of materials, while providing new insights into the nature of chemical bonding.

## AUTHOR INFORMATION

### Corresponding Author

*E-mail: Douglas.Keszler@oregonstate.edu.

## ACKNOWLEDGMENT

This material is based upon work supported by the National Science Foundation under Grant No. CHE-0847970 and by the U.S. Department of Energy, Office of Science, Office of Basic Energy Sciences under Contract No. DE-AC36-08GO28308 to NREL. The "Center for Inverse Design" is a DOE Energy Frontier Research Center.

## REFERENCES

(1) Bard, A. J.; Parsons, R.; Jordan, J. *Standard Potentials in Aqueous Solution*; Marcel Dekker: New York, 1985.

(2) van de Walle, C. G.; Neugebauer, J. *Nature* **2003**, *423* (6940), 626.

(3) Trasatti, S. *Pure Appl. Chem.* **1986**, *58*.

(4) In this article, SSE, EA, and IP are all expressed in units of eV (energy) and are referenced to the vacuum level so that they are negative quantities. Alternatively, they could be expressed in units of V (potential). If expressed in this manner, they would be positive quantities when referenced to the vacuum level.

(5) Shriver, D. F.; Atkins, P. W. *Inorg. Chem.* 3ed.; W.H. Freeman: New York, 1999.
(6) King, P. D. C.; Veal, T. D.; Fuchs, F.; Wang, C. Y.; Payne, D. J.; Bourlange, A.; Zhang, H.; Bell, G. R.; Cimalla, V.; Ambacher, O.; Egdell, R. G.; Bechstedt, F.; McConville, C. F. *Phys. Rev. B* **2009**, *79* (20), 205211.
(7) Dali, S. E.; Sunder, V. V. S. S.; Jayachandra, M.; Chockalingan, M. J. *J. Mat. Sci.* **1998**, *17*, 619.
(8) Barreau, N.; Marsillac, S.; Bernède, J. C.; Ben Nasrallah, T.; Belgacem, S. *Phys. Status Solidi a* **2001**, *184*, 179.
(9) Ruiz-Fuertes, J.; Errandonea, D.; Manjón, F. J.; Martínez-García, D.; Segura, A.; Ursaki, V. V.; Tiginyanu, I. M. *J. Appl. Phys.* **2008**, *103*, 063710.
(10) Pauling, L. *J. Am. Chem. Soc.* **1932**, *54* (9), 3570.
(11) Mulliken, R. S. *J. Chem. Phys.* **1934**, *2*.
(12) Huheey, J.; Keiter, E.; Keiter, R. *Inorganic Chemistry.: Principles of Structure and Reactivity*. 4 ed.; Prentice Hall: Upper Saddle River, NJ, 1997.
(13) Frese, K. W. *J. Vac. Sci. Technol.* **1979**, *16* (4), 1042.
(14) Ghosh, D. C.; Islam, N. *Int. J. Quantum Chem.* **2011**, *111* (1), 40.
(15) Bratsch, S. *J. Chem. Educ.* **1988**, *65*, 34.
(16) Pauling, L. *The Nature of the Chemical Bond*, 3ed.; Cornell University Press: Ithaca, NY, 1960.
(17) Pearson, R. G. *Chemical Hardness*; Wiley-VCH: Weinheim, Germany, 1997.
(18) Pearson, R. G. *J. Chem. Sci.* **2005**, *117*, 369.
(19) Phillips, J. C.; Lucovsky, G. *Bonds and Bands in Semiconductors.*, 2ed.; Momentum Press: New York, 2010.
(20) Harrison, W. *Elementary Electronic Structures*; World Scientific Publishing: River Edge, 1999.
(21) Brillson, L. J. *Surfaces and Interfaces of Electronic Matertials*; Wiley-VCH: Morlenbach, Germany, 2011.
(22) Predel, B.; Madelung, O. *Landolt-Bornstein, Electronic Materials and Semiconductors*; Springer - Verlag: Berlin, 2010.
(23) Adachi, S. *Handbook on Physical Properties of Semiconductors, Vols.* 1−3. Springer - Verlag: New York, 2004.
(24) Al-Kuhaili, M. F. *Opt. Mat.* **2004**, *27*, 383.
(25) Berger, L. *Semiconductor Materials*. CRC Press: Boca Raton, FL, 1997.
(26) Bozack, M. J. *Phys. Status Solidi B* **1997**, *202*, 549.
(27) Breeze, A. J.; Schlesinger, Z.; Carter, S. A.; Brock, P. J. *Phys. Rev. B* **2001**, *64* (12), 125205.
(28) Cogan, S. F.; Nguyen, N. M.; Perrotti, S. J.; Rauh, R. D. *J. Appl. Phys.* **1989**, *66* (3), 1333.
(29) Desai, S. R.; Wu, H.; Rohlfing, C. M.; Wang, L.-S. *J. Chem. Phys.* **1997**, *106* (4), 1309.
(30) Ebinghaus, H. Z. *Z. Naturforsch.* **1964**, *19A*, 727.
(31) Ferro, R.; Rodriguez, J. A. *Sol. Energy Mater. Sol. Cells* **2000**, *64*, 363.
(32) Fitz-Gerald, J. M.; Hoekstra, J.; Rack, P. D.; Fowlkes, J. D. *Appl. Phys. Let.* **2003**, *82* (20), 3466.
(33) Fonash, S. *Solar Cell Device Physics*, 2ed.; Academic Press: New York, 1981.
(34) Galtayries, A.; Wisniewski, S.; Grimblot, J. *J. Electron Spectrosc. Relat. Phenom.* **1997**, *87* (1), 31.
(35) Guo, L. *Comput. Mater. Sci.* **2008**, *42*, 489.
(36) Guo, L.; Wu, H. S. *Eur. Phys. J. D* **2007**, *42*, 259.
(37) Guo, Q.; Yoshida, A. *Jpn. J. Appl. Phys.* **1994**, *33*, 2453.
(38) Haynes, W. M., *CRC Handbook of Chemistry and Physics*: CRC Press: Boca Raton, FL, 2010; Vol. 91.
(39) Jefferson, P. H.; Hatfield, S. A.; Veal, T. D.; King, P. D. C.; McConville, C. F.; Zuniga Perez, J.; Munoz Sanjose, V. *Appl. Phys. Lett.* **2008**, *92* (2), 022101.
(40) Kaneko, Y.; Koda, T. *J. Cryst. Growth* **1990**, *86* (1−4), 72.
(41) Klein, A. *Appl. Phys. Let.* **2000**, *77* (13), 2009.
(42) Knapp, R. A. *Phys. Rev.* **1963**, *132* (5), 1891.
(43) Lai, B. C.-m.; Lee, J. Y.-m. *J. Electrochem. Soc.* **1999**, *146* (1), 266.
(44) Lehmann, W. *J. Electrochem. Soc.* **1970**, *117* (11), 1389.
(45) Levinshtein, M. E.; Shur, M.; Rumyantsev, S., *Properties of Advanced Semiconductor Materials: GaN, AlN, InN, BN, SiC, SiGe*. Wiley Interscience: Hoboken, NJ, 2001.
(46) Li, S. X.; Yu, K. M.; Wu, J.; Jones, R. E.; Walukiewicz, W.; Ager, J. W.; Shan, W.; Haller, E. E.; Lu, H.; Schaff, W. J. *Phys. Rev. B* **2005**, *71* (16), 161201.
(47) Madelung, O. *Semiconductors: Data Handbook*. 3ed.; Springer: New York, 2004.
(48) Martin, F. E.; Hensley, E. B. *Phys. Rev.* **1967**, *163* (2), 219.
(49) Monaghan, S.; Hurley, P. K.; Cherkaoui, K.; Negara, M. A.; Schenk, A. *Solid-State Electron.* **2009**, *53*, 438.
(50) Moormann, H.; Kohl, D.; Heiland, G. *Surf. Sci.* **1979**, *80*, 261.
(51) Peacock, P. W.; Robertson, J. *Appl. Phys. Let.* **2003**, *83* (10), 2025.
(52) Poole, R. T.; Jenkin, J. G.; Liesegang, J.; Leckey, R. C. G. *Phys. Rev. B* **1975**, *11*, 5179.
(53) Quiniou, B.; Schwarz, W.; Wu, Z.; Osgood, R. M.; Yang, Q.; Phillips, J. M. *Appl. Phys. Let.* **1992**, *60*, 183.
(54) Reynolds, K. J.; Barker, J. A.; Greenham, N. C.; Friend, R. H.; Frey, G. L. *J. Appl. Phys.* **2002**, *92* (12), 7556.
(55) Robertson, J. *J. Vac. Sci. Technol., B* **2000**, *18*, 1785.
(56) Strehlow, W. H.; Cook, E. L. *J. Phys. Chem. Ref. Data* **1973**, *2*, 163.
(57) Sze, S.; Ng, K. *Physics of Semiconductor Devices*, 2ed.; John Wiley and Sons: Hoboken, NJ, 2007.
(58) Teisseyre, H.; Perlin, P.; Suski, T.; Grzegory, I.; Porowski, S.; Jun, J.; Pietraszko, A.; Moustakas, T. D. *J. Appl. Phys.* **1994**, *76* (4), 2429.
(59) Thomas, T.; Guo, X.; Chandrashekhar, M. V. S.; Poitras, C. B.; Shaff, W.; Dreibelbis, M.; Reiherzer, J.; Li, K.; DiSalvo, F. J.; Lipson, M.; Spencer, M. G. *J. Cryst. Growth* **2009**, *311* (19), 4402.
(60) Tsou, K. Y.; Hensley, E. B. *J. Appl. Phys.* **1974**, *45*, 47.
(61) Wager, J. F.; Keszler, D. A.; Presley, R. E. *Transparent Electronics*; Springer: New York, 2008.
(62) Walter, C. W.; Hertzler, C. F.; Devynck, P.; Smith, G. P.; Peterson, J. R. *J. Chem. Phys.* **1991**, *95* (2), 824.
(63) Wang, L. S.; Wu, H.; Desai, S. L.; Fan, J.; Colson, S. D. *J. Phys. Chem.* **1996**, *100*, 8697.
(64) Wilk, G. D.; Wallace, R. M.; Anthony, J. M. *J. Appl. Phys.* **2001**, *89* (10), 5243.
(65) Williams, R. H.; Murray, R. B.; Govan, D. W.; Thomast, J. M.; Evans, E. L. *J. Phys. C: Solid State Phys.* **1973**, *6*, 3631.
(66) Zhai, H.-J.; Wang, L.-S. *J. Chem. Phys.* **2002**, *117* (17), 7882.
(67) Moore, C. E. *National Standard Reference Data Series*; National Bureau of Standards: Washington, DC, 1970; Vol. 34.
(68) Hotop, H.; Lineberger, W. C. *J. Phys. Chem. Ref. Data* **1985**, *68*, 731.
(69) Pearson, R. *Inorg. Chem.* **1988**, *27*, 734.
(70) Phillips, J. C. *Rev. Mod. Phys.* **1970**, *42*, 317.